

Dynamic response of a Timoshenko beam on a tensionless Pasternak foundation

İrfan Coşkun*¹, Hasan Engin² and Ayfer Tekin¹

¹Faculty of Civil Engineering, Yıldız Technical University, Davutpaşa Campus, 34210 Esenler, İstanbul, Turkey

²Faculty of Civil Engineering, İstanbul Technical University, 34469 Maslak, İstanbul, Turkey

(Received October 23, 2009, Accepted November 2, 2010)

Abstract. The dynamic response of a Timoshenko beam on a tensionless Pasternak foundation is investigated by assuming that the beam is subjected to a concentrated harmonic load at its middle. This action results in the creation of lift-off regions between the beam and the foundation that effect the character of the response. Although small displacements for the beam and the foundation are assumed, the problem becomes nonlinear since the contact/lift-off regions are not known at the outset. The governing equations of the beam, which are coupled in deflection and rotation, are obtained in both the contact and lift-off regions. After removing the coupling, the essentials of the problem (the contact regions) are determined by using an analytical-numerical method. The results are presented in figures to demonstrate the effects of some parameters on the extent of the contact lengths and displacements. The results are also compared with those of Bernoulli-Euler, shear, and Rayleigh beams. It is observed that the solution is not unique; for a fixed value of the frequency parameter, more than one solution (contact length) exists. The contact length of the beam increases with the increase of the frequency and rotary-inertia parameters, whereas it decreases with increasing shear foundation parameter.

Keywords: Timoshenko beam; Pasternak foundation; lift-off.

1. Introduction

The vibration, buckling, and bending problems of beams or beam-columns on elastic foundations are important in many fields of structural and foundation engineering. The Winkler model of elastic foundations is the most basic model, in which the foundation pressure at any point is proportional to the vertical deflection at that point (Hetényi 1946). The Winkler model represents the soil medium as a system of identical but mutually independent elastic springs. Although the model is simple and widely used, it does not accurately represent the characteristics of many practical foundations as the interactions between the springs are not considered. To overcome this problem, several two-parameter models have been suggested. Mathematically, all these models are equivalent and differ only in their definitions of the foundation parameters (Selvadurai 1979, Dutta and Roy 2002). In this paper, Pasternak's model has been employed to represent the soil foundation, in which shear interaction between the springs is considered. This is accomplished by connecting the top ends of

*Corresponding author, Ph.D., E-mail: coskun@yildiz.edu.tr

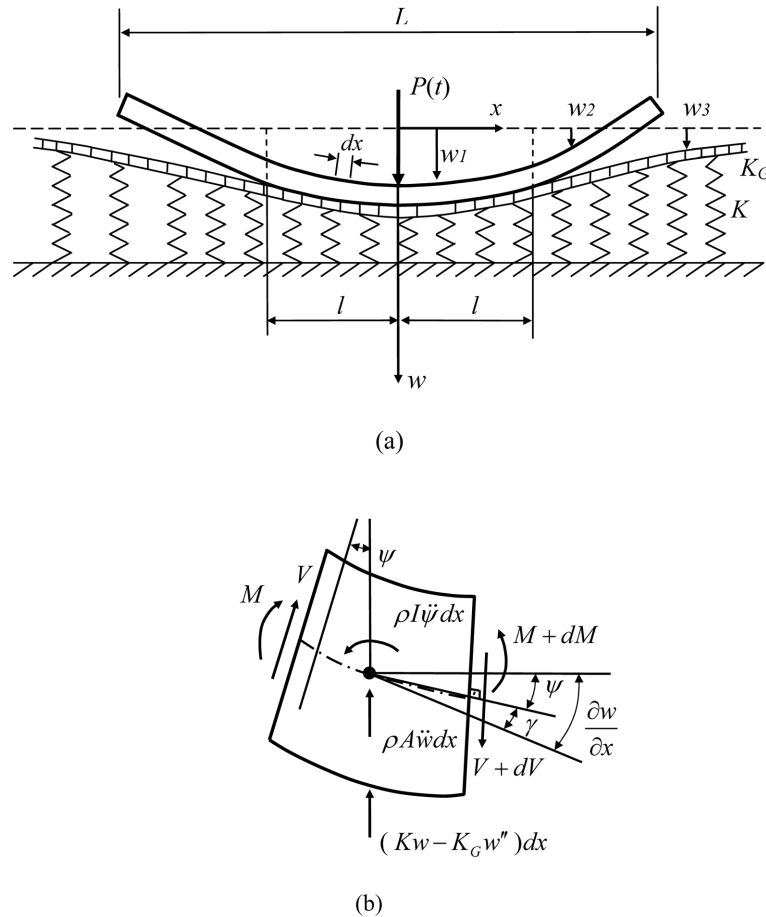


Fig. 1 (a) A Timoshenko beam resting on a tensionless Pasternak foundation subjected to a harmonic load, (b) Forces, moments, and deformations on the differential element

the springs to an incompressible layer that resists only transverse deformation (Fig. 1(a)).

A number of studies have investigated the dynamic responses of beams and beam-columns on two-parameter elastic foundations within the scope of classical Bernoulli-Euler beam theory (Eisenberger and Clastornik 1987, Valsangkar and Pradhanang 1988, Karamanlidis and Prakash 1989, Franciosi and Masi 1993, De Rosa and Maurizi 1998, Filipich and Rosales 2002, Rao 2003, Mallik *et al.* 2006), and using Timoshenko beam theory (Wang and Stephens 1977, Wang and Gagnon 1978, Filipich and Rosales 1988, Yokoyama 1991, De Rosa 1995, El-Mously 1999, Kargarnovin and Younesian 2004, Arboleda-Monsalve *et al.* 2008). In these studies, the problems have been analyzed by assuming that the foundation reacts in tension as well as in compression. This assumption that the contact between the beam and the foundation is established continuously simplifies the problem. However, in several engineering applications, the foundation can not provide tensile reactions and, under certain conditions, some parts of the beam may lift-off. Therefore, a one-way or tensionless foundation, which reacts to compressive stresses but is incapable of experiencing tension, should be used for realistic results. The problem of beams resting on a

tensionless foundation is complicated because the contact region, which appears as the primary unknown in the governing equations, is not known in advance. Thus, even for cases involving linear foundation models and linear beam theories, the problem is nonlinear and needs to be solved iteratively. Studies on this subject have mainly been concerned with the determination of the location, magnitude, and extent of the lift-off region(s), as well as the beam deflection at any point.

The static response of infinite beams resting on a tensionless Winkler foundation subjected to a concentrated load and to a uniformly distributed load was studied by Tsai and Westmann (1967), Weitsman (1970), and Ioakimidis (1996). For more complex loads and tensionless Pasternak foundation, a similar study was carried out by Ma *et al.* (2009). The dynamic response of an infinite beam resting on a tensionless foundation and subjected to a moving load was studied by Weitsman (1971). The same problem, but for different configurations, was studied by Choros and Adams (1979) and by Lin and Adams (1987). The response of finite beams on tensionless foundations has been considered in various studies. Kerr and Coffin (1991), for example, studied the response of free beams resting on a tensionless Pasternak foundation subjected to a concentrated central load. Zhang and Murphy (2004) and Silveira *et al.* (2008) studied the response of free-free and pinned-pinned beams on a tensionless Winkler foundation for different loading cases. Celep and Demir (2005) studied the behaviour of a rigid beam on a tensionless two-parameter elastic foundation subjected to a concentrated load and a moment. The same authors also studied the response of an elastic beam on such a foundation by considering a uniformly distributed load and concentrated edge loads (Celep and Demir 2007). Recently, the response of a pinned-pinned beam resting on a tensionless Reissner foundation under symmetric and asymmetric loading was studied by Zhang (2008). By considering the same loading case but a tensionless Pasternak foundation, the response of a free-free beam was studied by Coşkun *et al.* (2008). These studies dealt with static loading conditions. Studies involving dynamic behaviour of finite beams on the one and-two parameter tensionless elastic foundation do appear in the literature. Celep *et al.* (1989), for example, studied the forced vibrations of a free beam resting on a tensionless Winkler foundation under the combined actions of concentrated and uniformly distributed loads and external moments. Coşkun and Engin (1999) and Coşkun (2003) studied the harmonic vibrations of a free beam on a nonlinear tensionless Winkler and tensionless Pasternak foundation subjected to a concentrated load, respectively. Finally, Lancioni and Lenci (2007) studied nonlinear vibrations of a semi-infinite beam on a tensionless Winkler foundation subjected to a uniformly distributed load. However, in these studies the formulations were based on the Bernoulli-Euler beam theory, and therefore the effects of rotatory inertia and shear deformation are not accounted for. These effects, which are important for short beams and beams where higher modes are excited, can be taken into account by using the well-known Timoshenko beam model. According to the authors' knowledge, there have been no studies addressing the dynamic response of Timoshenko beams on a tensionless elastic Pasternak-type foundation.

In this paper, the dynamic response of a finite Timoshenko beam resting on a tensionless Pasternak foundation is investigated. The beam is subjected to a concentrated harmonic load at the centre. The study is carried out by assuming that the beam separates from the foundation symmetrically. Closed-form solutions of the differential equations of motion in each of the contact and noncontact regions are determined by using trigonometric-hyperbolic functions. The boundary and continuity conditions are then satisfied, which leads to a system of algebraic equations that are linear in certain unknown coefficients and nonlinear in the unknown contact region lengths. With the elimination of the linear coefficients, the contact and noncontact lengths are obtained

numerically from the resulting transcendental equation by using the Newton Raphson technique. Numerical results are presented in dimensionless graphical form to illustrate the effect of some parameters on the extent of the contact lengths and the vertical displacements of the beam.

2. Formulation of the problem

Consider a Timoshenko beam of length L resting on a tensionless elastic foundation subjected to a concentrated central load $P(t) = P_0 \exp(i\Omega t)$ as shown in Fig. 1(a). Since the foundation is assumed to be tensionless, the beam can lift off the foundation at the points $x = \pm l$. The elastic foundation is idealized as a two-parameter Pasternak model characterized by two moduli, the Winkler foundation modulus K and the shear foundation modulus K_G . The forces and the deformations of a differential beam element are shown in Fig. 1(b). All the symbols shown in this figure are defined as follows: w , γ , and ψ represent the deflection, shear distortion, and bending rotation of the beam, ρ , I , and A represent the beam material density, second moment of area, and cross-sectional area of the beam, and V and M represent the shear force and bending moment at any beam section, respectively. In the present formulation, the normal inertia and damping of the foundation are neglected. Also, it is assumed that both the beam and foundation are isotropic, homogeneous and linearly elastic, and the vibration amplitudes of the system are sufficiently small. The governing equations are derived by applying the basic concepts of dynamic equilibrium on the differential element shown in Fig. 1(b). The transverse and rotational equilibrium equations are

$$\frac{\partial V}{\partial x} = \rho A \frac{\partial^2 w}{\partial t^2} + Kw - K_G \frac{\partial^2 w}{\partial x^2} \quad (1)$$

and

$$\frac{\partial M}{\partial x} = V - \rho I \frac{\partial^2 \psi}{\partial t^2} \quad (2)$$

From Fig. 1(b), the shear distortion can be expressed as

$$\gamma = \frac{\partial w}{\partial x} - \psi \quad (3)$$

The bending moment and the shear force are then computed from the familiar relations

$$M = -EI \frac{\partial^2 w}{\partial x^2} = -EI \frac{\partial \psi}{\partial x} \quad (4)$$

$$V = GAk^* \gamma = GAk^* \left(\frac{\partial w}{\partial x} - \psi \right) \quad (5)$$

in which E and G are the modulus of elasticity and shear modulus, respectively, and k^* is the sectional shear coefficient. Substituting Eqs. (4) and (5) into Eqs. (1) and (2), utilizing symmetry, and denoting the vertical displacements and rotations as w_1, ψ_1 and w_2, ψ_2 in the contact and noncontact regions, respectively, the following differential equations are obtained

$$GAk^* \left(\frac{\partial \psi_1}{\partial x} - \frac{\partial^2 w_1}{\partial x^2} \right) + \rho A \frac{\partial^2 w_1}{\partial t^2} + Kw_1 - K_G \frac{\partial^2 w_1}{\partial x^2} = P_0 e^{i\Omega t} \delta(x), \quad 0 < x < l \quad (6)$$

$$GAk^* \left(\frac{\partial w_1}{\partial x} - \psi_1 \right) + EI \frac{\partial^2 \psi_1}{\partial x^2} = \rho I \frac{\partial^2 \psi_1}{\partial t^2}, \quad 0 < x < l \quad (7)$$

$$GAk^* \left(\frac{\partial \psi_2}{\partial x} - \frac{\partial^2 w_2}{\partial x^2} \right) + \rho A \frac{\partial^2 w_2}{\partial t^2} = 0, \quad l < x < L/2 \quad (8)$$

$$GAk^* \left(\frac{\partial w_2}{\partial x} - \psi_2 \right) + EI \frac{\partial^2 \psi_2}{\partial x^2} = \rho I \frac{\partial^2 \psi_2}{\partial t^2}, \quad l < x < L/2 \quad (9)$$

in which P_0 , Ω , $\delta(x)$, and l are the magnitude of the load, the forcing frequency, the Dirac delta function, and the extent of the unknown contact region, respectively. These equations, which govern the dynamic behaviour of the beam, are second-order differential equations coupled in w_1 and ψ_1 (also in w_2 and ψ_2). On the other hand, the governing equation of the free foundation surface (see Fig. 1(a)) can be written as (Kerr and Coffin 1991)

$$Kw_3 - K_G \frac{\partial^2 w_3}{\partial x^2} = 0, \quad l < x < \infty \quad (10)$$

Since the forcing is harmonic in time, and thus the response of the beam and the foundation is harmonic, the displacement and rotation can be written as

$$w_i(x, t) = W_i(x) e^{i\Omega t}, \quad \psi_i(x, t) = \Psi_i(x) e^{i\Omega t}, \quad i = 1, 2 \quad (11)$$

where $W_i(x)$ and $\Psi_i(x)$ represent the shape functions. For convenience, the nondimensionalized variable ξ , displacement $W(\xi)$, rotation $\Psi(\xi)$, contact length X , Winkler foundation constant λ_w , shear (Pasternak) foundation constant λ_p , beam rotary-inertia parameter R , beam shearing-flexibility parameter S , frequency parameter Ω_f , and applied load parameter F_0 , are introduced as follows

$$\xi = \frac{x}{L}, \quad W(\xi) = \frac{W(x)}{L}, \quad \Psi(\xi) = \frac{\Psi(x)}{L}, \quad X = \frac{l}{L}, \quad \lambda_w = \frac{KL^4}{EI}, \quad \lambda_p = \frac{K_G L^2}{EI}$$

$$R^2 = \frac{I}{AL^2}, \quad S^2 = \frac{EI}{GAk^* L^2}, \quad \Omega_f^2 = \frac{\rho AL^4}{EI} \Omega^2, \quad F_0 = \frac{P_0 L^2}{EI} \quad (12)$$

Introducing Eqs. (11) and (12) into Eqs. (6)-(10), and removing the coupling between the displacement and rotation in Eqs. (6) and (7) (also, in Eqs. (8) and (9)), one obtains the following nondimensional equations for W and Ψ

$$(1 + S^2 \lambda_p) \frac{d^4 W_1(\xi)}{d\xi^4} - [\lambda_p + S^2 \lambda_w - \Omega_f^2 (S^2 + R^2 + R^2 S^2 \lambda_p)] \frac{d^2 W_1(\xi)}{d\xi^2}$$

$$+ [\lambda_w + \Omega_f^2 (R^2 S^2 \Omega_f^2 - 1 - R^2 S^2 \lambda_w)] W_1(\xi) = F_0 \delta(\xi), \quad 0 < \xi < X \quad (13)$$

$$(1+S^2\lambda_p)\frac{d^4\Psi_1(\xi)}{d\xi^4}-[\lambda_p+S^2\lambda_w-\Omega_f^2(S^2+R^2+R^2S^2\lambda_p)]\frac{d^2\Psi_1(\xi)}{d\xi^2} \\ +[\lambda_w+\Omega_f^2(R^2S^2\Omega_f^2-1-R^2S^2\lambda_w)]\Psi_1(\xi)=0, \quad 0<\xi<X \quad (14)$$

$$\frac{d^4W_2(\xi)}{d\xi^4}+[\Omega_f^2(S^2+R^2)]\frac{d^2W_2(\xi)}{d\xi^2}+[\Omega_f^2(R^2S^2\Omega_f^2-1)]W_2(\xi)=0, \quad X<\xi<\frac{1}{2} \quad (15)$$

$$\frac{d^4\Psi_2(\xi)}{d\xi^4}+[\Omega_f^2(S^2+R^2)]\frac{d^2\Psi_2(\xi)}{d\xi^2}+[\Omega_f^2(R^2S^2\Omega_f^2-1)]\Psi_2(\xi)=0, \quad X<\xi<\frac{1}{2} \quad (16)$$

$$\lambda_p\frac{d^2W_3(\xi)}{d\xi^2}-\lambda_wW_3(\xi)=0, \quad X<\xi<+\infty \quad (17)$$

Notice that if the effect of rotatory inertia is neglected ($R=0$) and only the effect of shear deformation is considered, Eqs. (13)-(16) represent the behaviour of a shear beam on the tensionless Pasternak foundation. If only the effect of rotatory inertia is considered and the effect of shear is neglected ($S=0$), the Rayleigh model is the result. If we neglect both the effect of shear and the effect of rotatory inertia ($R=0, S=0$), we obtain the classical Bernoulli-Euler beam model. Moreover, for $R=S=\lambda_p=0$, these equations represent the behaviour of a Bernoulli-Euler beam on a tensionless Winkler foundation. The boundary and continuity conditions in dimensionless form are as follows

$$(i) \text{ at point } \xi=0: \quad L\Psi_1(0)=0, \quad \frac{dW_1(0)}{d\xi_1}-L\Psi_1(0)=\frac{F_0}{2}S^2 \quad (18a)$$

$$(ii) \text{ at point } \xi=X: \quad W_1(X)=W_2(X), \quad W_1(X)=W_3(X), \quad \frac{dW_1(X)}{d\xi}=\frac{dW_3(X)}{d\xi} \\ L\Psi_1(X)=L\Psi_2(X), \quad L\frac{d\Psi_1(X)}{d\xi}=L\frac{d\Psi_2(X)}{d\xi} \\ \frac{dW_1(X)}{d\xi}-L\Psi_1(X)=\frac{dW_2(X)}{d\xi}-L\Psi_2(X) \quad (18b)$$

$$(iii) \text{ at point } \xi=\frac{1}{2}: \quad L\frac{d\Psi_2\left(\frac{1}{2}\right)}{d\xi}=0, \quad \frac{dW_2\left(\frac{1}{2}\right)}{d\xi}-L\Psi_2\left(\frac{1}{2}\right)=0 \quad (18c)$$

$$(iv) \lim_{\xi \rightarrow +\infty} \{W_3(\xi)\} \rightarrow \text{finite} \quad (18d)$$

Eq. (18a) is due to the symmetry assumption. Eq. (18b) is the geometric and natural boundary conditions that require the continuity of the displacement, slope, rotation, bending moment, and shear force at the separation point X . Eq. (18c) represents the natural boundary conditions at the free and unloaded end of the beam, indicating that there is no moment or shear force at that point.

Finally, Eq. (18d) physically states that the displacements of the free foundation surface approach zero as ξ gets larger.

In the formulation given above, it is assumed that the ends of the beam separate from the foundation. However, in some cases, the beam may be completely compressed into the foundation (no separation develops). In this complete contact case, the slope of the foundation surface at the beam ends will have discontinuity. Thus, the boundary conditions that will be satisfied at $\xi = 1/2$ are

$$W_1\left(\frac{1}{2}\right) = W_3\left(\frac{1}{2}\right), \quad L \frac{d\Psi_1\left(\frac{1}{2}\right)}{d\xi} = 0, \quad \lambda_p \left(\frac{dW_1\left(\frac{1}{2}\right)}{d\xi} - \frac{dW_3\left(\frac{1}{2}\right)}{d\xi} \right) + \frac{1}{S^2} \left(\frac{dW_1\left(\frac{1}{2}\right)}{d\xi} - L\Psi_1\left(\frac{1}{2}\right) \right) = 0 \quad (19)$$

The third boundary condition is the force equilibrium at the end of the beam between the foundation concentrated force and the shearing force of the beam. In addition to the complete contact case, the beam may separate from the foundation completely or contact and non-contact regions may interchange as the excitation is harmonic. When the beam separates from the foundation completely, the governing equation of the beam for deflections becomes $W''''(\xi) + \Omega_f^2(R^2 + S^2)W'''(\xi) + \Omega_f^2(R^2S^2\Omega_f^2 - 1)W(\xi) = F_0\delta(\xi)$, and can be solved with the appropriate boundary/continuity conditions and the jump condition on the shear. When the contact and non-contact regions interchange (i.e., the middle part of the beam lifts off the foundation while the ends of the beam make contact with the foundation), it is necessary to reformulate the problem with different boundary/continuity conditions. These conditions are given in the Appendix.

3. Solution

Eqs. (13) and (14) are, respectively, fourth order nonhomogeneous and homogeneous differential equations with constant coefficients. However, Eq. (13) can be put in a homogeneous form, and the external load can be treated as a jump in the shear force and can be included in the boundary conditions. The solution of these homogeneous equations is of the form $W_1(\Psi_1) = Ce^{m\xi}$. Substituting this solution into Eq. (13) or (14), one obtains the following characteristic polynomial

$$m^4 - bm^2 + c = 0 \quad (20)$$

where $b = [\lambda_p + S^2\lambda_w - \Omega_f^2(S^2 + R^2 + R^2S^2\lambda_p)]/r$ and $c = [\lambda_w + \Omega_f^2(R^2S^2\Omega_f^2 - 1 - R^2S^2\lambda_w)]/r$ with $r = (1 + S^2\lambda_p)$. It is clear that the solutions of Eqs. (13) and (14) depend on the nature of the characteristic roots ($m_i, i = 1-4$) of Eq. (20). Defining $\Delta_1 = b^2 - 4c$, the following cases can be distinguished with $i = \sqrt{-1}$

$$(a) \quad \Delta_1 > 0, \quad \sqrt{\Delta_1} > b \Rightarrow m_{1,2} = \pm\gamma, \quad m_{3,4} = \pm i\mu$$

$$W_1(\xi) = A_1 \cosh \gamma\xi + A_2 \sinh \gamma\xi + A_3 \cos \mu\xi + A_4 \sin \mu\xi \quad (21a)$$

$$\Psi_1(\xi) = B_1 \cosh \gamma\xi + B_2 \sinh \gamma\xi + B_3 \cos \mu\xi + B_4 \sin \mu\xi \quad (21b)$$

$$(b) \Delta_1 > 0, b > 0, \sqrt{\Delta_1} < b \Rightarrow m_{1,2} = \pm\gamma, m_{3,4} = \pm\theta$$

$$W_1(\xi) = A_1 \cosh \gamma\xi + A_2 \sinh \gamma\xi + A_3 \cosh \theta\xi + A_4 \sinh \theta\xi \quad (22a)$$

$$\Psi_1(\xi) = B_1 \cosh \gamma\xi + B_2 \sinh \gamma\xi + B_3 \cosh \theta\xi + B_4 \sinh \theta\xi \quad (22b)$$

$$(c) \Delta_1 > 0, b < 0, \sqrt{\Delta_1} < |b| \Rightarrow m_{1,2} = \pm i\mu, m_{3,4} = \pm ip$$

$$W_1(\xi) = A_1 \cos \mu\xi + A_2 \sin \mu\xi + A_3 \cos p\xi + A_4 \sin p\xi \quad (23a)$$

$$\Psi_1(\xi) = B_1 \cos \mu\xi + B_2 \sin \mu\xi + B_3 \cos p\xi + B_4 \sin p\xi \quad (23b)$$

$$(d) \Delta_1 = 0, b > 0 \Rightarrow m_{1,2} = \sqrt{b/2}, m_{3,4} = -\sqrt{b/2}$$

$$W_1(\xi) = (A_1 + A_2\xi)e^{(\sqrt{b/2})\xi} + (A_3 + A_4\xi)e^{-(\sqrt{b/2})\xi} \quad (24a)$$

$$\Psi_1(\xi) = (B_1 + B_2\xi)e^{(\sqrt{b/2})\xi} + (B_3 + B_4\xi)e^{-(\sqrt{b/2})\xi} \quad (24b)$$

$$(e) \Delta_1 = 0, b < 0 \Rightarrow m_{1,2} = i\sqrt{b/2}, m_{3,4} = -i\sqrt{b/2}$$

$$W_1(\xi) = (A_1 + A_2\xi) \cos \sqrt{b/2} \xi + (A_3 + A_4\xi) \sin \sqrt{b/2} \xi \quad (25a)$$

$$\Psi_1(\xi) = (B_1 + B_2\xi) \cos \sqrt{b/2} \xi + (B_3 + B_4\xi) \sin \sqrt{b/2} \xi \quad (25b)$$

$$(f) \Delta_1 < 0 \Rightarrow m_{1,2,3,4} = \pm(\alpha \pm i\eta)$$

$$W_1(\xi) = (A_1 \cosh \alpha\xi + A_2 \sinh \alpha\xi) \cos \eta\xi + (A_3 \cosh \alpha\xi + A_4 \sinh \alpha\xi) \sin \eta\xi \quad (26a)$$

$$\Psi_1(\xi) = (B_1 \cosh \alpha\xi + B_2 \sinh \alpha\xi) \cos \eta\xi + (B_3 \cosh \alpha\xi + B_4 \sinh \alpha\xi) \sin \eta\xi \quad (26b)$$

In Eqs. (21)-(26), A_i and B_i ($i = 1-4$) are the integration constants, and the parameters $\gamma, \mu, \theta, p, \alpha$, and η are defined by $\gamma = \sqrt{(b + \sqrt{\Delta_1})/2}, \mu = \sqrt{(-b + \sqrt{\Delta_1})/2}, \theta = \sqrt{(b - \sqrt{\Delta_1})/2}, p = \sqrt{(-b - \sqrt{\Delta_1})/2}, \alpha = \sqrt{b/4 + \sqrt{c/4}}$, and $\eta = \sqrt{-b/4 + \sqrt{c/4}}$. Eqs. (15) and (16) are also fourth order homogeneous differential equations with constant coefficients. Thus, the solution can be sought in the form $W_2(\Psi_2) = De^{n\xi}$. After substituting into Eq. (15) or (16), the following polynomial is obtained

$$n^4 + dn^2 + e = 0 \quad (27)$$

where $d = \Omega_f^2(S^2 + R^2)$ and $e = \Omega_f^2(R^2S^2\Omega_f^2 - 1)$. The solutions of Eqs. (15) and (16) depend on the nature of the characteristic roots (n_i ($i = 1-4$)) of Eq. (27). Defining $\Delta_2 = d^2 - 4e$, the following cases can be distinguished with $i = \sqrt{-1}$

(g) $\Delta_2 > 0, \sqrt{\Delta_2} > d \Rightarrow n_{1,2} = \pm\chi, n_{3,4} = \pm i\beta$

$$W_2(\xi) = C_1 \cosh \chi\xi + C_2 \sinh \chi\xi + C_3 \cos \beta\xi + C_4 \sin \beta\xi \tag{28a}$$

$$\Psi_2(\xi) = D_1 \cosh \chi\xi + D_2 \sinh \chi\xi + D_3 \cos \beta\xi + D_4 \sin \beta\xi \tag{28b}$$

(h) $\Delta_2 > 0, \sqrt{\Delta_2} < d \Rightarrow n_{1,2} = \pm iq, n_{3,4} = \pm i\beta$

$$W_2(\xi) = C_1 \cos q\xi + C_2 \sin q\xi + C_3 \cos \beta\xi + C_4 \sin \beta\xi \tag{29a}$$

$$\Psi_2(\xi) = D_1 \cos q\xi + D_2 \sin q\xi + D_3 \cos \beta\xi + D_4 \sin \beta\xi \tag{29b}$$

(i) $\Delta_2 = 0 \Rightarrow n_{1,2} = i\sqrt{d/2}, n_{3,4} = -i\sqrt{d/2}$

$$W_2(\xi) = (C_1 + C_2\xi) \cos \sqrt{d/2} \xi + (D_3 + D_4\xi) \sin \sqrt{d/2} \xi \tag{30a}$$

$$\Psi_2(\xi) = (D_1 + D_2\xi) \cos \sqrt{d/2} \xi + (D_3 + D_4\xi) \sin \sqrt{d/2} \xi \tag{30b}$$

In Eqs. (28)-(30), C_i and $D_i (i = 1-4)$ are the integration constants, and the parameters $\chi, \beta,$ and q are defined by $\chi = \sqrt{(-d + \sqrt{\Delta_2})/2}, \beta = \sqrt{(d + \sqrt{\Delta_2})/2},$ and $q = \sqrt{(d - \sqrt{\Delta_2})/2}.$ Note that the case $\Delta_2 < 0$ does not exist in the solution. Finally, the solution of Eq. (17), which represents the vertical displacements of the free part of the foundation surface, is given by

$$W_3(\xi) = E_1 e^{-s\xi} + E_2 e^{s\xi} \tag{31}$$

where $s = \sqrt{\lambda_w/\lambda_p}.$

There are a total of 18 unknown constants ($A_i, B_i, C_i, D_i (i = 1-4)$ and $E_j (j = 1-2)$) in these equations. However, the constants A_i and B_i are not independent, but are related by Eq. (6). The dimensionless form of this equation is

$$-\left(\frac{1}{S^2} + \lambda_p\right) \frac{d^2 W_1}{d\xi^2} + \frac{L}{S^2} \frac{d\Psi_1}{d\xi} + (\lambda_w - \Omega_f^2) W_1 = 0 \tag{32}$$

Substituting the sets of solutions (a)-(f) into Eq. (32), the constants B_i can be obtained in terms of the constants $A_i.$ For example, substituting Eqs. (21a) and (21b) into Eq. (32) shows that

$$B_1 = (\bar{\gamma}/L)A_2, \quad B_2 = (\bar{\gamma}/L)A_1, \quad B_3 = (\bar{\mu}/L)A_4, \quad B_4 = -(\bar{\mu}/L)A_3 \tag{33}$$

where $\bar{\gamma} = [(1 + S^2 \lambda_p)\gamma^2 + S^2(\Omega_f^2 - \lambda_w)]/\gamma$ and $\bar{\mu} = [(1 + S^2 \lambda_p)\mu^2 + S^2(\lambda_w - \Omega_f^2)]/\gamma.$ In addition, the constants C_i and D_i are not independent, but are related by Eq. (8). The dimensionless form of this equation is

$$-\frac{1}{S^2} \frac{d^2 W_2}{d\xi^2} + \frac{L}{S^2} \frac{d\Psi_2}{d\xi} - \Omega_f^2 W_1 = 0 \tag{34}$$

Substituting the sets of solutions (g)-(i) into Eq. (34), the constants D_i can be obtained in terms of the constants C_i . As before, substituting Eqs. (28a) and (28b) into Eq. (34), for example, shows that

$$D_1 = (\bar{\chi}/L)C_2, \quad D_2 = (\bar{\chi}/L)C_1, \quad D_3 = (\bar{\beta}/L)C_4, \quad D_4 = -(\bar{\beta}/L)C_3 \quad (35)$$

where $\bar{\chi} = (\chi^2 + S^2\Omega_f^2)/\chi$ and $\bar{\beta} = (\beta^2 - S^2\Omega_f^2)/\beta$. Due to these relations, the number of unknown constants for the contact and noncontact regions reduces to 8. Thus, we have 10 constants (2 of them are due to Eq. (31)). In addition to these constants, the separation point X is also unknown. Hence, there are a total of 11 unknowns to be determined. These unknowns can be determined using the boundary and continuity conditions given by Eqs. (18) (there are 11). At first glance, this may appear to be a simple linear boundary problem. However, because the separation point X appears in the argument to the solution, the problem is nonlinear. Hence, the problem is solved numerically by applying an iterative scheme as follows. First, the boundary and continuity conditions are satisfied, which leads to a system of algebraic equations that are linear in certain unknown integral constants and nonlinear in the unknown separation point. Then, eliminating the linear integral constants, the separation point (contact length) is determined from the resulting transcendental equation using the Newton-Raphson technique. During the numerical calculations, the vertical equilibrium of the beam is controlled at every step by considering

$$\frac{F_0}{2} = \int_0^X [-\lambda_p W_1''(\xi) + (\lambda_w - \Omega_f^2) W_1(\xi)] d\xi - \Omega_f^2 \int_X^{1/2} W_2(\xi) d\xi \quad (36)$$

With the separation point determined, the deflections of the beam and the free foundation surface can be calculated in a straightforward manner. It should be noted here that the response of the system is harmonic due to the harmonic excitation. So, the system composed of Eqs. (13)-(17) presents the steady motion of a Timoshenko beam resting on a two-parameter elastic foundation subjected to a harmonic load with an excitation frequency Ω . Therefore, the contact lengths and displacements obtained from the steady solutions given in Sec. 3 are independent of time, but they depend on the frequency parameter Ω_f and the other system parameters.

4. Numerical results and discussion

Numerical results are presented in this section for a Timoshenko beam subjected to a central harmonic load and resting on a tensionless Pasternak foundation. In addition, some comparisons are made by considering Rayleigh, shear, and Bernoulli-Euler beams. Since the analysis of the problem depends on many parameters ($E, G, A, I, k^*, \rho, F_0, L, l, K, K_G, \Omega$), a parametric study is conducted to investigate the effects of the rotary-inertia, shear foundation modulus and the forcing frequency on the contact lengths and displacements of the beam. In all numerical computations, the shear correction factor and Poisson's ratio for the beam are taken to be $k^* = 5/6$ (rectangular cross section) and $\nu = 1/3$ ($E/G = 8/3$), respectively. For these parameters, the relation between S and R can be obtained as $S^2 = 3.2R^2$ (see Eqs. (12)). The values of R are chosen between 0.02 and 0.10 to show the differences among the above mentioned models. These values correspond to small slenderness ratios (non-slender beams) as the slenderness ratio can be taken as the inverse of R . The

foundation parameters (λ_p and λ_w) used in the work of Yokoyama (1991) were selected for the numerical computations as $\lambda_p = 0, 1, 5, 10$ and 25 ($\cong \pi^2 \times \lambda_G, \lambda_G = kL^4 / \pi^2 EI$); λ_w values varying from 1 to 10^6 . Note that $\lambda_p = 0$ corresponds to the usual Winkler model assumption. On the other hand, the real foundation parameters K and K_G appeared in Eq. (1) are based on the constrained deformation of an elastic layer given by Vlasov and Leont'ev (1966). For a single layer of thickness H with a linear variation of normal stresses, these parameters are given by $K = E_s/H(1 + \nu_s)(1 - 2\nu_s)$, $K_G = E_s H/6(1 + \nu_s)$. The values of E_s (the elastic modulus of the soil) and ν_s (the Poisson's ratio of the soil) can be determined from triaxial tests.

Finally, in order to diminish the number of parameters, the first foundation parameter in the Pasternak foundation model is assumed to be constant at $\lambda_w = 1000$, and the applied load is taken to be $F_0 = 1$ (except in Fig. 7).

Fig. 2 shows the variation of the separation point (contact length) X with respect to the frequency parameter Ω_f for some values of the rotary-inertia parameter R . The shear foundation parameter is selected as $\lambda_p = 25$. As seen in the figure, the contact length of the beam increases with an increase of the frequency parameter. With the increase of Ω_f , first one and then two solutions (two different contact lengths at a fixed frequency) appear in the system. In other words, the solution is not unique; for a given beam length and frequency more than one solution exists. The stability of the solutions are not investigated here, but the actual solution can be obtained by using an energy criterion. As is expected, the nonuniqueness of the solution is due to the nonlinear character of the problem. With further increases in the frequency parameter, contact lengths reach the beam length ($X = 1/2$) and complete contact develops in the system for the first solution (upper curves in the figure). However, for the second solution (lower curves in the figure), the beam continues to

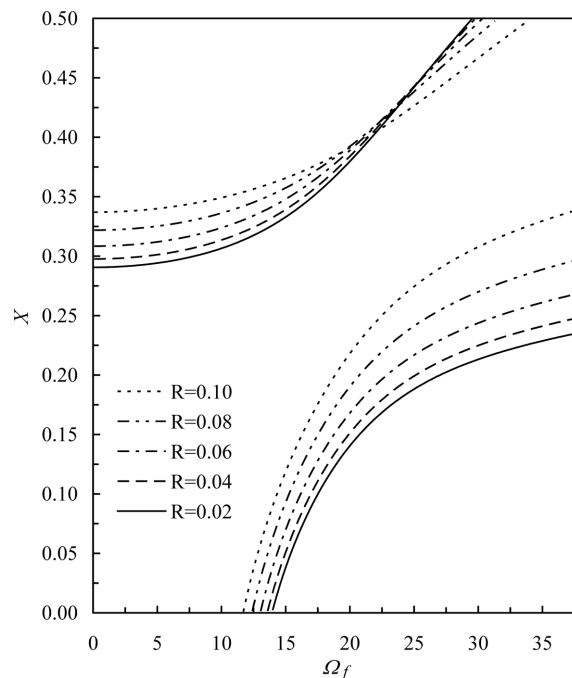


Fig. 2 Contact length versus frequency parameter for various values of the rotary-inertia parameter with $\lambda_p = 25$. The upper and lower curves correspond to the first and second solutions, respectively

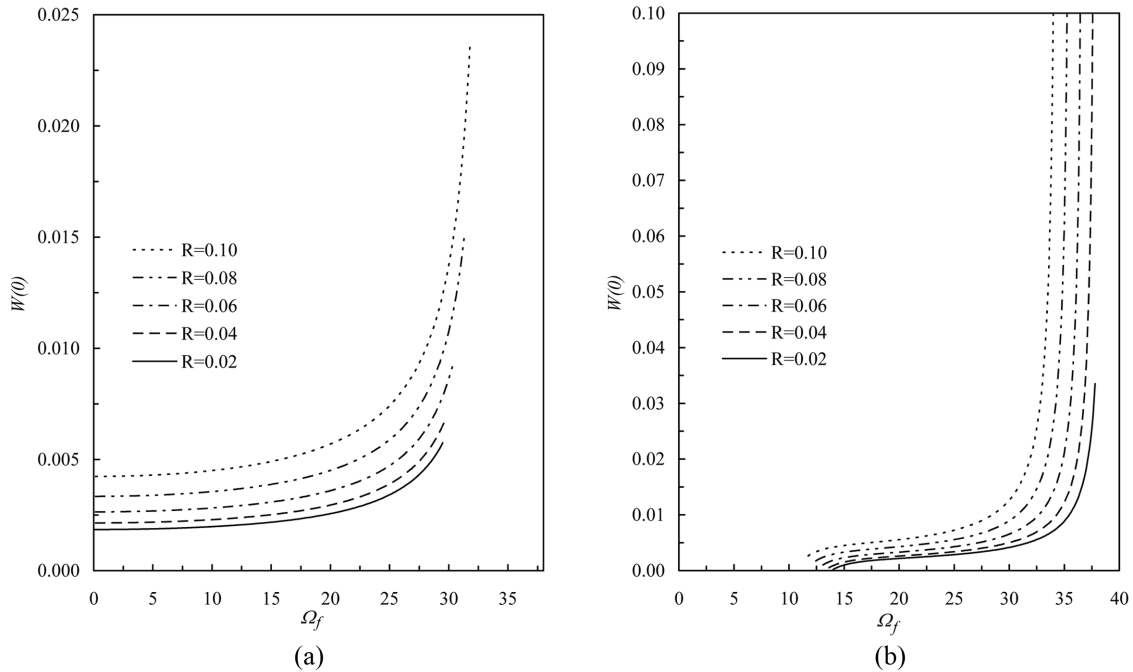


Fig. 3 Middle displacement versus frequency parameter for various values of the rotary-inertia parameter with $\lambda_p = 25$ (a) First solution, (b) Second solution

separate from the foundation until about $\Omega_f = 38$. When Ω_f increased beyond this value, the beam deflections significantly increase and the contact and non-contact regions are interchanged. In other words, the middle part of the beam lifts off the foundation while the two sides make contact with the foundation. In this case, it is necessary to reformulate the problem with different boundary and continuity conditions, which are given in the Appendix. Fig. 2 also shows the effect of R on the contact length of the beam. As is seen, contact length increases with the increase of R for both of the solutions.

Figs. 3(a) and (b) show the middle displacements of the beam corresponding to the upper and lower contact curves (the first and the second solutions) given in Fig. 2, respectively. As is seen, displacements increase as frequency and rotational inertia increase for both of the solutions. As the frequency is increased further, the displacements greatly increase (Fig. 3(b)) and the contact and noncontact regions interchange as was described above. The effect of the rotational inertia on the displacements and the contact length of the beam at a fixed frequency ($\Omega_f = 20$) can clearly be seen in Fig. 4. The contact length of the beam and the displacements increase with the increase of rotational inertia. This agrees with Figs. 2 and 3(b). Fig. 5 shows the variation of the contact length with respect to the frequency parameter for some values of the shear foundation parameter λ_p . The rotary-inertia parameter is selected as $R = 0.04$. As seen in the figure, two solutions for the system exist, and the contact lengths of the beam increase as frequency increases. However, the contact lengths decrease with the increase of λ_p as the foundation becomes stiffer. Note that the case $\lambda_p = 0$ corresponds to the Winkler foundation idealization.

The variation of the middle displacements with respect to the frequency parameter is given in Figs. 6(a) and (b) for the first and second solutions, respectively. It is seen that the displacements

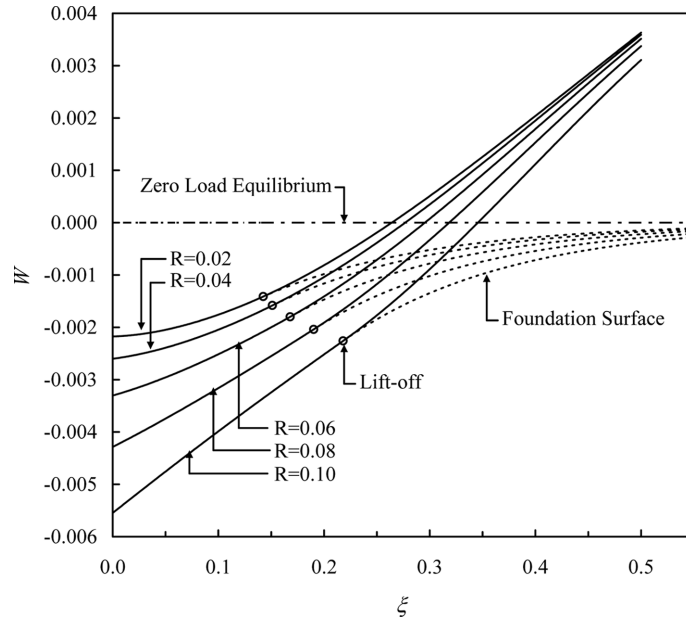


Fig. 4 Deflection curves showing lift-off for various values of the rotary-inertia parameter with $\lambda_p = 25$ and $\Omega_f = 20$, for the second solution

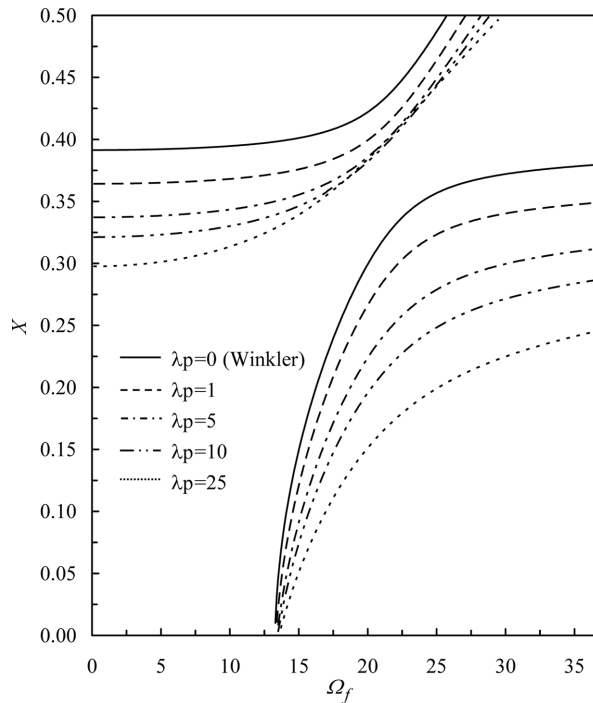


Fig. 5 Contact length versus frequency parameter for various values of the shear foundation parameter with $R = 0.04$. The upper and lower curves correspond to the first and second solutions, respectively

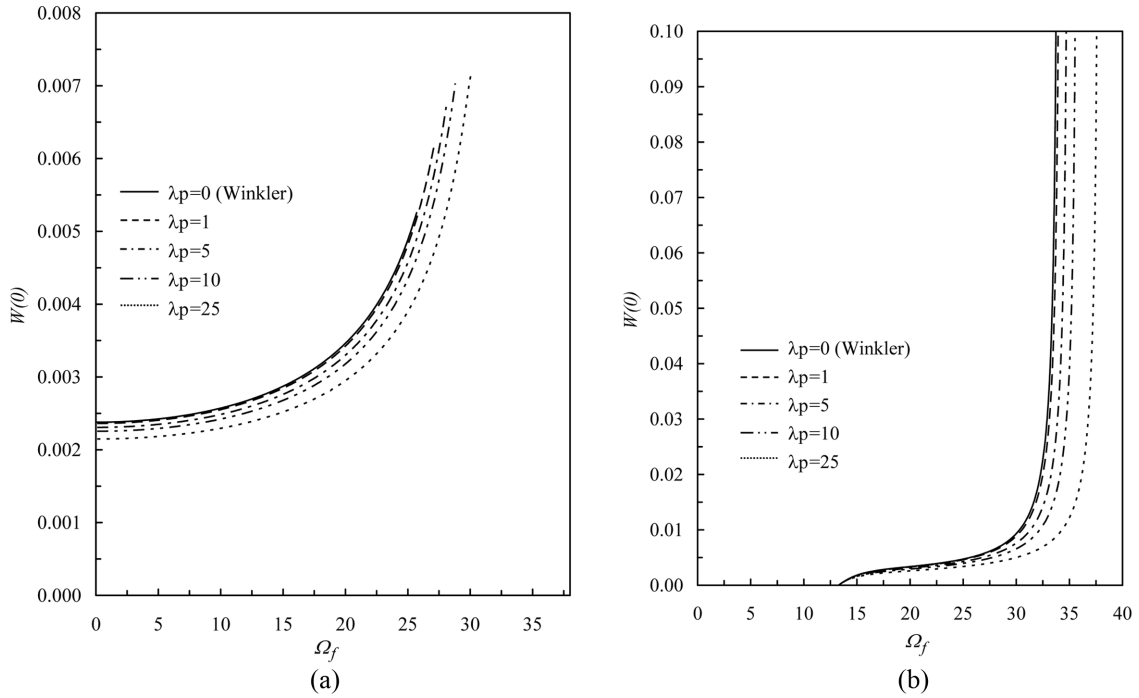


Fig. 6 Middle displacement versus frequency parameter for various values of the shear foundation parameter with $R = 0.04$ (a) First solution, (b) Second solution

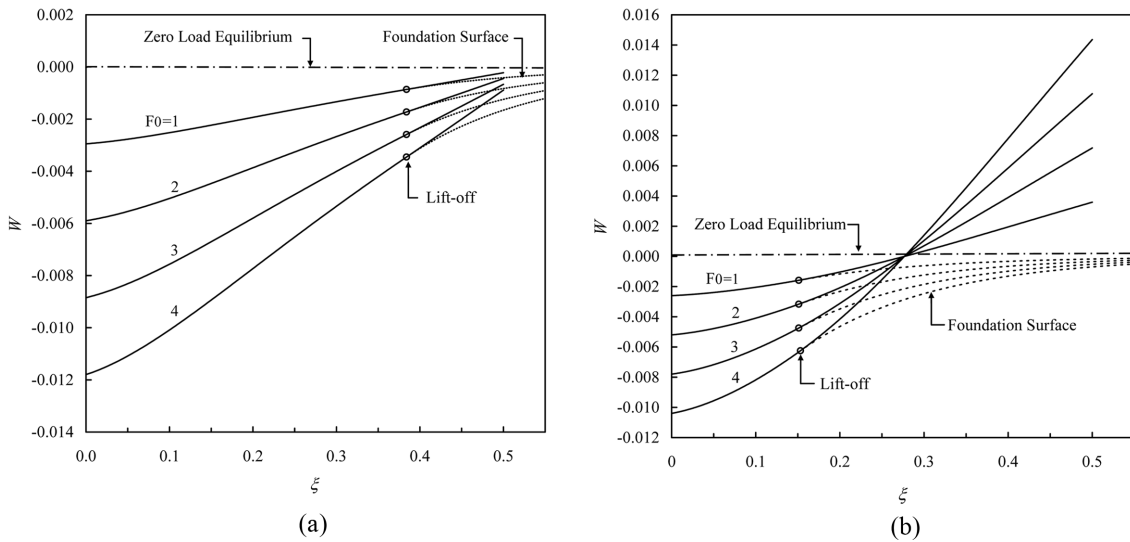


Fig. 7 Deflection curves showing lift-off for different loads with $R = 0.04$, $\Omega_f = 20$ and $\lambda_p = 25$ (a) First solution, (b) Second solution

increase with increasing frequency, whereas they decrease with increasing the foundation parameter λ_p . Also, with further increases in the frequency, the displacements greatly increase for the second solution (for the lower contact curves given in Fig. 5) as seen in Fig. 6(b), and the contact and

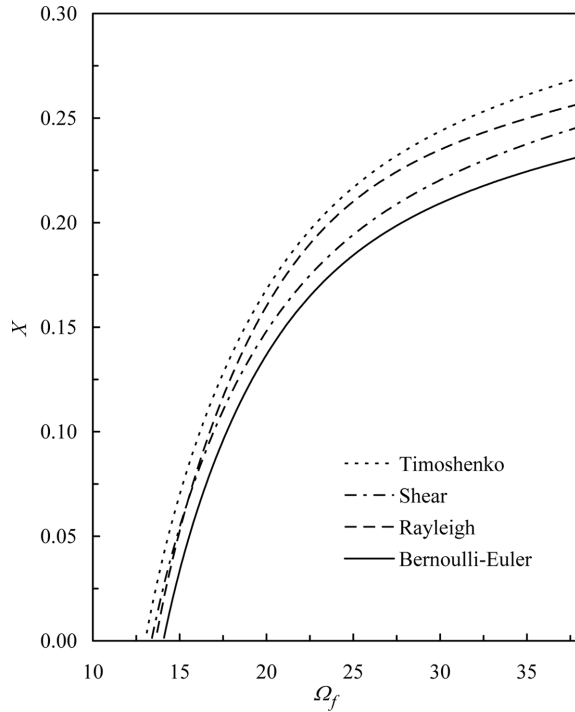


Fig. 8 Contact length versus frequency parameter for different beam models with $R = 0.06$ and $\lambda_p = 25$

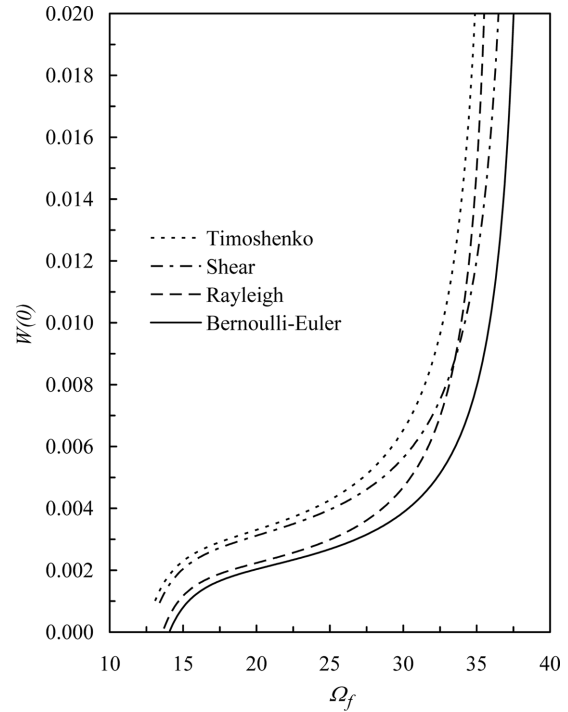


Fig. 9 Middle displacement versus frequency parameter for different beam models with $R = 0.06$ and $\lambda_p = 25$

noncontact regions interchange as was described before. Fig. 7 shows the deflections of the beam and the foundation surface under different loads, $F_0 = 1, 2, 3, 4$, for $R = 0.04$, $\Omega_f = 20$, and $\lambda_p = 25$. It also highlights the existence of two solutions (i.e., two different contact lengths for the same parameters) in the problem. The contact lengths of the beam for the first and second solutions are $X = 0.383$ (Fig. 7(a)) and $X = 0.151$ (Fig. 7(b)), respectively. Figs. 7(a) and (b) show that the displacements increase with the increase of load. However, the extent of the contact length does not change, i.e., it is independent of the magnitude of the applied load.

All the results given above deal with the response of the Timoshenko beam in which the rotatory inertia and shear deformations are accounted for. The variations of the contact length and the middle displacement with the frequency parameter for various beam models are given in Figs. 8 and 9, respectively. The contact lengths and the middle displacements increase as the frequency increases for all beam models. The rotatory inertia and the shear deformation effects have significant influences on both the extent of the contact lengths and the displacements. As is seen in Fig. 8, the contact length of the Timoshenko beam is greater than the contact lengths of the other beams. The Bernoulli-Euler beam ($R = 0, S = 0$) has the smallest contact length. As is expected, the Rayleigh ($S = 0$) and shear beam ($R = 0$) contact lengths are between those of the above mentioned cases. Notice that if only the effect of rotatory inertia is considered (Rayleigh beam), the contact length is smaller than that of the shear beam for small values of Ω_f . However, with the increase of Ω_f , the effect of the rotatory inertia becomes dominant, and a larger contact length is obtained for the Rayleigh beam. A similar trend is observed for the middle displacements, as shown in Fig. 9.

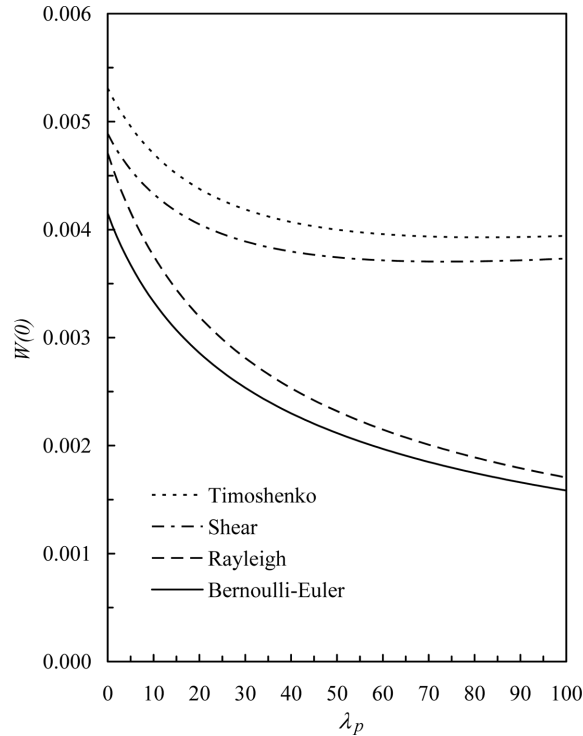


Fig. 10 Middle displacement versus shear foundation parameter for different beam models with $R = 0.06$ and $\Omega_f = 25$

Finally, Fig. 10 shows the variation of the middle displacements with respect to the shear foundation parameter λ_p for various beam models with $\Omega_f = 25$ and $R = 0.06$. Displacement decreases as λ_p increases for all beam models. This is due to the stiffening effect caused by the shear layer of the two-parameter model of the foundation. A comparison of Fig. 10 with Fig. 9 shows that at a fixed value of Ω_f or λ_p , the solutions for the Rayleigh and shear beams are between those of the Timoshenko and Bernoulli-Euler beams.

5. Conclusions

The lift-off problem of a free Timoshenko beam resting on a tensionless Pasternak foundation and subjected to a concentrated harmonic load at the centre was investigated in this paper. Bernoulli-Euler, Rayleigh, and shear beams were also studied for comparison. Closed-form solutions of the differential equations, which depend on the system parameters, were obtained in both the contact and lift-off regions. Due to the nonlinear character of the problem, the essentials of the problem (the lift-off points) were determined numerically. From the numerical analysis, the following conclusions can be drawn:

(1) The extent of the contact lengths and the vertical displacements of the Timoshenko beam change considerably with the frequency parameter. The increase in the value of this parameter increases the contact lengths and the displacements of the beam. Depending on the values of this

parameter, more than one solution (contact length) may exist in the system, i.e., the solution is not unique. The nonuniqueness of the solutions is due to the nonlinearity associated with the existence of the lift-off regions.

(2) The influence of the beam rotary-inertia parameter on the response is found to be significant. The increase in the value of this parameter increases the extent of the contact lengths and displacements. For a Timoshenko beam, these quantities are greater than those of the Bernoulli-Euler, shear, and Rayleigh beams. The Bernoulli-Euler beam solution gives the smallest contact lengths and displacements. These results show that the combined effects of the rotatory inertia and shear deformation changes the response of the beam considerably. As is shown, if only one of these effects is considered, the solutions are between those of the Timoshenko and Bernoulli-Euler beams.

(3) The shear foundation parameter also has a significant effect on the response. In contrast to the effect of the rotary-inertia parameter, an increase in the value of this parameter decreases the contact lengths and displacements of the beam. This is due to the stiffening effect caused by the shear layer of the Pasternak foundation model.

(4) The contact length of the Timoshenko beam is independent of the amplitude of the external load, whereas the deflection profile is directly proportional to it. This holds for not only for the Timoshenko beam but also for the Bernoulli-Euler, shear, and Rayleigh beams.

References

- Arboleda-Monsalve, L.G., Zapata-Medina, D.G. and Aristizabal-Ochoa, J.D. (2008), "Timoshenko beam-column with generalized end conditions on elastic foundation: Dynamic-stiffness matrix and load vector", *J. Sound Vib.*, **310**, 1057-1079.
- Celep, Z. and Demir, F. (2005), "Circular rigid beam on a tensionless two-parameter elastic foundation", *ZAMM-Z. Angew. Math. Me.*, **85**(6), 431-439.
- Celep, Z. and Demir, F. (2007), "Symmetrically loaded beam on a two-parameter tensionless foundation", *Struct. Eng. Mech.*, **27**(5), 555-574.
- Celep, Z., Malaika, A. and Abu-Hussein, M. (1989), "Forced vibrations of a beam on a tensionless foundation", *J. Sound Vib.*, **128**, 235-246.
- Choros, J. and Adams, G.G. (1979), "A steadily moving load on an elastic beam resting on a tensionless Winkler foundation", *J. Appl. Mech.-ASME*, **46**(1), 175-180.
- Coşkun, İ. and Engin, H. (1999), "Non-linear vibrations of a beam on an elastic foundation", *J. Sound Vib.*, **223**(3), 335-354.
- Coşkun, İ. (2003), "The response of a finite beam on a tensionless Pasternak foundation subjected to a harmonic load", *Eur. J. Mech. A-Solids*, **22**, 151-161.
- Coşkun, İ., Engin, H. and Özmutlu, A. (2008), "Response of a finite beam on a tensionless Pasternak foundation under symmetric and asymmetric loading", *Struc. Eng. Mech.*, **30**(1), 21-36.
- De Rosa, M.A. (1995), "Free vibrations of Timoshenko beams on two-parameter elastic foundation", *Comput. Struct.*, **57**(1), 151-156.
- De Rosa, M.A. and Maurizi, M.J. (1998), "The influence of concentrated masses and Pasternak soil on the free vibrations of Euler beams-exact solution", *J. Sound Vib.*, **212**(4), 573-581.
- Dutta, S.C. and Roy, R. (2002), "A critical review on idealization and modeling for interaction among soil-foundation-structure system", *Comput. Struct.*, **80**, 1579-1594.
- Eisenberger, M. and Clastornik, J. (1987), "Beams on variable two-parameter elastic foundation", *J. Eng. Mech.-ASCE*, **113**(10), 1454-1466.
- El-Mously, M. (1999), "Fundamental frequencies of Timoshenko beams mounted on Pasternak foundation", *J. Sound Vib.*, **228**(2), 452-457.
- Filipich, C.P. and Rosales, M.B. (1988), "A variant of Rayleigh's method applied to Timoshenko beams

- embedded in a Winkler-Pasternak medium”, *J. Sound Vib.*, **124**(3), 443-451.
- Filipich, C.P. and Rosales, M.B. (2002), “A further study about the behaviour of foundation piles and beams in a Winkler-Pasternak soil”, *Int. J. Mech. Sci.*, **44**(1), 21-36.
- Franciosi, C. and Masi, A. (1993), “Free vibrations of foundation beams on two-parameter elastic soil”, *Comput. Struct.*, **47**(3), 419-426.
- Hetényi, M. (1946), *Beams on Elastic Foundation*, The University of Michigan Press, Ann Arbor, MI.
- Ioakimidis, N.I. (1996), “Beams on tensionless elastic foundation: Approximate quantifier elimination with Chebyshev series”, *Int. J. Numer. Meth. Eng.*, **39**(4), 663-686.
- Karamanlidis, D. and Prakash, V. (1989), “Exact transfer and stiffness matrices for a beam/column resting on a two-parameter foundation”, *Comput. Meth. Appl. Mech. Eng.*, **72**, 77-89.
- Kargarnovin, D. and Younesian, D. (2004), “Dynamics of Timoshenko beams on Pasternak foundation under moving load”, *Mech. Res. Commun.*, **31**, 713-723.
- Kerr, A.D. and Coffin, D.W. (1991), “Beams on a two-dimensional Pasternak base subjected to loads that cause lift-off”, *Int. J. Solids Struct.*, **28**(4), 413-422.
- Lancioni, G. and Lenci, S. (2007), “Forced nonlinear oscillations of a semi-infinite beam resting on a unilateral elastic soil: Analytical and numerical solutions”, *J. Comput. Nonlin. Dyn.-ASME*, **2**(2), 155-166.
- Lin, L. and Adams, G.G. (1987), “Beam on tensionless elastic foundation”, *J. Eng. Mech.-ASCE*, **113**(4), 542-553.
- Ma, X., Butterworth, J.W. and Clifton, G.C. (2009), “Static analysis of an infinite beam resting on a tensionless Pasternak foundation”, *Eur. J. Mech. A-Solids*, **28**, 697-703.
- Mallik, A.K., Chandra, S. and Singh, A.B. (2006), “Steady-state response of an elastically supported infinite beam to a moving load”, *J. Sound Vib.*, **291**, 1148-1169.
- Rao, G.V. (2003), “Large-amplitude free vibrations of uniform beams on Pasternak foundation”, *J. Sound Vib.*, **263**(4), 954-960.
- Selvadurai, A.P.S. (1979), *Elastic Analysis of Soil-Foundation Interaction*, Elsevier, Amsterdam.
- Silveira, R.A.M., Pereira, W.L.A. and Gonçalves, P.B. (2008), “Nonlinear analysis of structural elements under unilateral contact constraints by a Ritz type approach”, *Int. J. Solids Struct.*, **45**, 2629-2650.
- Tsai, N.C. and Westmann, R.E. (1967), “Beams on tensionless foundation”, *J. Eng. Mech. Div.-ASCE*, **93**, 1-12.
- Valsangkar, A.J. and Pradhanang, R. (1988), “Vibrations of beam-columns on two-parameter elastic foundations”, *Earthq. Eng. Struct. D.*, **16**, 217-225.
- Vlasov, V.Z. and Leont’ev, U.N. (1966), *Beams, Plates and Shells on Elastic Foundation* (Translated from Russian), Israel Program for Scientific Translations, Jerusalem.
- Wang, T.M. and Gagnon, M.J. (1978), “Vibrations of continuous Timoshenko beams on Winkler-Pasternak foundations”, *J. Sound Vib.*, **59**(2), 211-220.
- Wang, T.M. and Stephens, J.E. (1977), “Natural frequencies of Timoshenko beams on Pasternak foundations”, *J. Sound Vib.*, **51**(2), 149-155.
- Weitsman, Y. (1970), “On foundations that react in compression only”, *J. Appl. Mech.-ASME*, **37**(4), 1019-1030.
- Weitsman, Y. (1971), “Onset of separation between a beam and tensionless elastic foundation under a moving load”, *Int. J. Mech. Sci.*, **13**, 707-711.
- Yokoyama, T. (1991), “Vibrations of Timoshenko beam-columns on two-parameter elastic foundations”, *Earthq. Eng. Struct. D.*, **20**(4), 355-370.
- Zhang, Y. (2008), “Tensionless contact of a finite beam resting on Reissner foundation”, *Int. J. Mech. Sci.*, **50**, 1035-1041.
- Zhang, Y. and Murphy, D.K. (2004), “Response of a finite beam in contact with a tensionless foundation under symmetric and asymmetric loading”, *Int. J. Solids Struct.*, **41**, 6745-6758.

Appendix

The boundary and continuity conditions for the case when the contact and non-contact regions interchange are as follows

$$(i) \text{ at point } \xi = 0 : \quad L\Psi_1(0) = 0, \quad \frac{dW_1(0)}{d\xi_1} - L\Psi_1(0) = \frac{F_0}{2}S^2, \quad \frac{dW_4(0)}{d\xi} = 0$$

$$(ii) \text{ at point } \xi = X : \quad W_1(X) = W_2(X), \quad W_1(X) = W_4(X), \quad \frac{dW_1(X)}{d\xi} = \frac{dW_4(X)}{d\xi}$$

$$L\Psi_1(X) = L\Psi_2(X), \quad L\frac{d\Psi_1(X)}{d\xi} = L\frac{d\Psi_2(X)}{d\xi}$$

$$\frac{dW_1(X)}{d\xi} - L\Psi_1(X) = \frac{dW_2(X)}{d\xi} - L\Psi_2(X)$$

$$(iii) \text{ at point } \xi = \frac{1}{2} : \quad W_2\left(\frac{1}{2}\right) = W_3\left(\frac{1}{2}\right), \quad L\frac{d\Psi_2(\frac{1}{2})}{d\xi} = 0,$$

$$\lambda_p \left(\frac{dW_2(\frac{1}{2})}{d\xi} - \frac{dW_3(\frac{1}{2})}{d\xi} \right) + \frac{1}{S^2} \left(\frac{dW_2(\frac{1}{2})}{d\xi} - L\Psi_2\left(\frac{1}{2}\right) \right) = 0$$

$$(iv) \quad \lim_{\xi \rightarrow +\infty} \{W_3(\xi)\} \rightarrow \text{finite}$$

Here, W_1 and W_4 are the vertical deflections of the beam and shear layer in the non-contact region (i.e., in the middle part of the beam), respectively; W_2 is the beam deflection in the contact region; W_3 is the deflection of the shear layer in the region $1/2 < \xi < \infty$. Note that the number of the boundary and continuity conditions becomes 13 for this case.